Phase Stabilized Design of a Hard Disk Drive Servo Using the Complex Lag Compensator

William Messner and Roberto Oboe

Abstract— **This paper introduces a new technique for the Phase Stabilized Design (PSD) of a HDD servo, based on the use of complex lag compensators. Such compensators have several benefits compared to standard ones and they offer additional degrees of freedom in control design. This paper presents a case study comparing the performance of the PSD using the complex lag compensator with the performance of a PID plus notch filter design, and the performance of a PSD using a real lag compensator. The designs are performed for a realistic model of a disk drive derived from experimental data. The new approach significantly outperforms the other with respect to step response, rejection of disturbance response at the plant input, and rejection of periodic and windage disturbances.**

I. Introduction

HIGH capacity in modern Hard Disk Drives (HDDs) has been reached by wisely combining several technological improvements. Modern disk drives have better magnetic materials, smoother bearings, more sensitive heads and flatter disks, and head positioning systems with increased bandwidth and disturbance rejection capabilities. This paper concerns the design of high performance servo-controllers, with a larger bandwidth compared to the existing solutions.

The major impediment to increasing bandwidth is the presence of mechanical resonances in the head servo-positioning equipment. Such resonances are due to the flexible elements in the mechanical system, e.g. the VCM pivot support, the VCM arm and the head suspension. The first resonant mode is usually the pivot bending mode. Attempts to enlarge the servo bandwidth cause lightly damped oscillations near the frequency of this mode to appear in the time response. Dual stage actuation and phase stabilized design are two approaches to addressing to this limitation. Dual stage actuation can extend the overall bandwidth of the head servo-positioning system, but the costs of the manufacturing and retooling and potential reliability problems have kept the technology out of products, so far.

William Messner is with Carnegie Mellon University, 5000 Forbes Avenue Pittsburgh, PA 15213-3890, USAPhone: +1- 412-268-2510 Fax: +1-412-268-3348 email: bmessner@andrew.cmu.edu

Roberto Oboe is with Department of Mechanical and Structural Engineering, University of Trento, via Mesiano 77, 38050 Trento – Italy Phone: +39-0461-882584 Fax: +39-0461-882599 e-mail: roberto.oboe@ing.unitn.it

The Phase Stabilized Design (PSD) tries to improve the performance of single actuator systems by modifying the design of the standard servo controller. We briefly recall here the principles behind this technique. Figure 1 shows a simplified frequency response of a HDD VCM, characterized by two low-frequency real poles, and two high frequency complex poles of the first mechanical resonance.

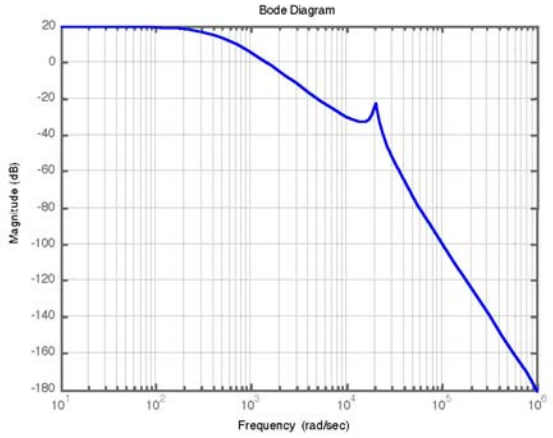

Figure 1 – Simplified VCM transfer function

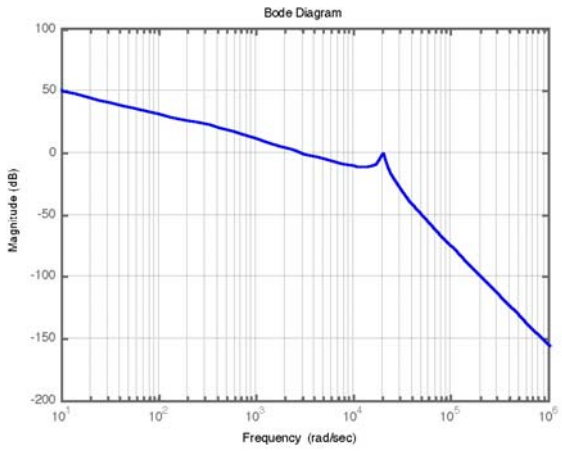

Figure 2 – Mode spillover with PID control

A simple approach for the servo controller design is to use a standard PID controller, tuned to achieve a certain open loop crossing frequency and a desired phase margin at that frequency. Enlarging the closed loop bandwidth by

increasing the 0 dB crossing frequency while maintaining the phase margin can lead to multiple crossings of the loop transfer function, due to the presence of lightly damped resonant modes, as shown in Fig.2. Cascading a notch filter with the PID controller can eliminate the multiple 0 dB crossings, but this notch reduces disturbance rejection and causes phase warping that adversely affects the overall servo performance.

An alternative approach to dealing with the effects of mechanical resonances employs the so-called "secondary phase margin", which is defined when the open loop has multiple 0 dB crossings [1]. The concept is easily understood by examining the Nyquist plot of Figure 3. The damping of the resonance in closed-loop depends on the secondary phase margin.

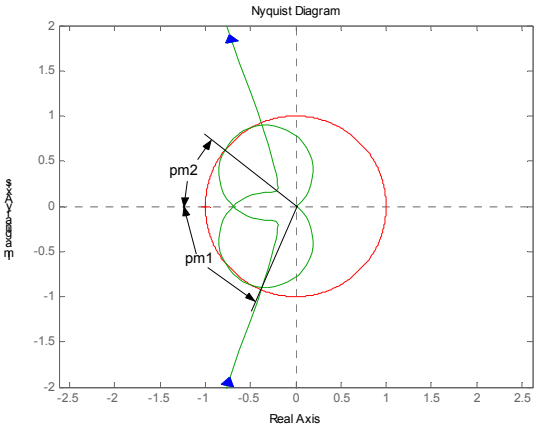

Figure 3 – Primary and secondary phase margin definition

The secondary phase margin is the clockwise angular distance *pm2* from the negative real axis and the second crossing of the unit circle. The distance from the critical point and the secondary crossing is |1+L|, and L has a unity gain at crossing. The magnitude of the sensitivity function |1/(1+L)| and the magnitude of the complementary sensitivity function |L/(1+L)| will both be large in the vicinity of the crossing frequency, if the secondary phase margin is small. Consequently, there will be a peak in the closed-loop frequency response, and the time response will be oscillatory.

Phase Stabilized Design explicitly addresses this limitation, by using a phase-shaping network to increase the secondary phase margin, while maintaining a high primary crossing frequency and, in turn, a large closed loop bandwidth. Typical phase-shaping networks are properly tuned lag compensators, which move the secondary crossing point clockwise in the Nyquist plot by reducing both the phase and the gain of the loop transfer function after the first crossing. A limitation of this approach is that the gain and phase characteristic standard lag-lead compensators also alter both the primary crossing frequency and the primary phase margin. If the lag compensator is realized with real pole-zero pairs, the servo designer has little freedom in the overall design, since the maximum phase lag is a function of the ratio of the pole to the zero [3].

This paper presents a solution for the PSD of a HDD servo-controller, in which a lag compensator with complex conjugate zeros and poles shapes the phase and gain profile after the first 0 dB crossing. These complex lag compensators, introduced in [3] as lead compensators, can introduce a phase lag with a narrower profile, compared to standard lag compensators with real zeros and poles. Moreover, large phase variations can be obtained without introducing large gain variations outside the close neighbourhood of the secondary crossing frequency.

The paper is organized as follows. Section II describes the plant characteristics. Section III presents three designs—a PID plus notch compensator design for use as a benchmark for other designs, a standard PSD with a real lag, and a PSD with complex lag. Performance comparisons of the three controllers evaluated in an accurate simulation environment [2] appear in Section IV. Section V concludes the paper with some final remarks.

II. PLANT CHARACTERISTICS AND SERVO DESIGN SPECIFICATIONS

The model used for this design study is based on an actual disk drive. Figure 4 shows a HDD modified for LDV measurement of the head, and Figure 5 shows the magnitude of the frequency response from current command to head position. Figure 5 also shows the frequency response of a 22nd order model, obtained by a least squares fit to frequency response data by using MATLAB *invfreqs* command. Table 1 gives the frequencies and damping ratios of the modes of the model. The experimental equipment was also used to collect repeatable runout (RRO) and non-repeatable runout (NRRO) data from the disk drive for use as inputs in the simulations comparing the performance of the various controllers.

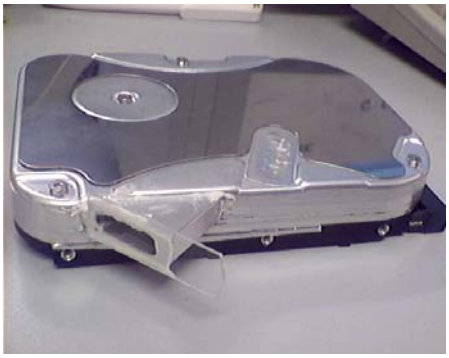

Figure 4 – Modified disk for VCM transfer function identification.

The discrete time designs reported in the following section used a sampling period of T_s=35 μs, which is typical for recent low-end HDDs. The block diagram in Figure 6

depicts the servo-positioning system for the VCM, where R(z) represents the discrete time controller and PA(s) represents the power amplifier dynamics. The delay is placed at the input of the controlled plant. The design process ignored the phase lag due to the transconductance amplifier (50 kHz bandwidth) and the Td = 5 μs delay due to A/D conversion, computation, and D/A conversion. However, the simulation of the responses of the closed-loop for each design included these dynamics.

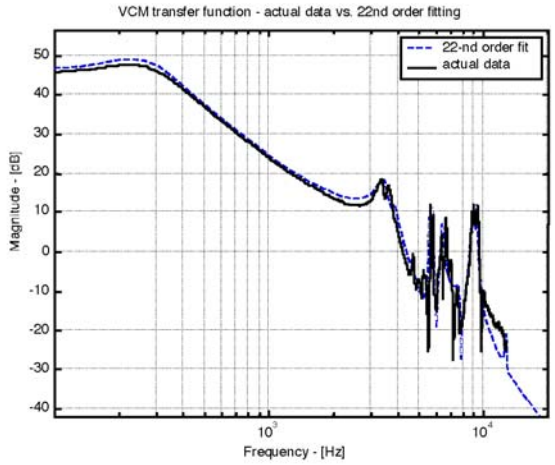

Figure 5– Frequency response of experimental data and of 22nd order model.

TABLE I
MODES FREQUENCIES AND DAMPING RATIOS

Frequency	Damping ratio	Frequency	Damping ratio
279	0.38	7,781	0.018
3,481	0.032	8,928	0.0096
3,821	0.028	9,409	0.0052
5,662	0.0022	9,522	0.0074
5,832	0.0027	12,886	0.0044
6,440	0.012		

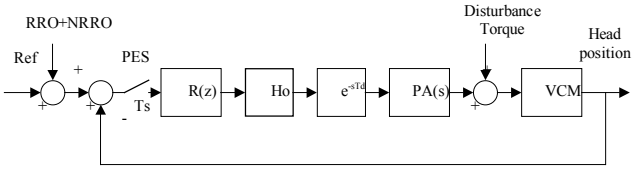

Figure 6 – Head position servo-control system – Block diagram

Table 2 lists the design specifications as follows:

TABLE I
SERVO-CONTROLLER DESIGN SPECIFICATIONS

Crossing frequency	maximize
Primary phase margin	≥ 60 deg
Secondary phase margin	≥ 60 deg
Gain margin	≥ 6 dB

Of course, standard the PID design allows for the specification of the primary phase margin, only.

III. SERVO DESIGN

This section describes the design of three different compensators for the plant model of Section II. All three designs of this paper employed a PID compensator of the following form:

$$C_{pid}(s) = k\frac{s^2 + 2(0.707)\omega_n s + \omega_n^2}{s(s+100\omega_n)} \qquad (1)$$

which was then converted to discrete-time using frequency pre-warping at the natural frequency ω_n. The PID plus notch design first employed two notch filters of the form

$$C_{notch}(s) = \frac{s^2 + 2(0.707)\omega_{notch} s + \omega_{notch}^2}{s^2 + 2(0.0707)\omega_{notch} s + \omega_{notch}^2} \qquad (2)$$

before conversion to discrete-time with frequency pre-warping at the notch frequencies. These compensators provided a 20 dB notch at while minimizing the phase loss at lower frequencies. The notch frequencies were 3,342 Hz and 9,390 Hz corresponding to the most prominent resonant modes in the plant. The natural frequency of the PID was chosen to be 239 Hz to achieve a 0 dB crossover at 500 Hz with 60 degrees of phase margin, while assuring that no resonance peak was greater than –9.5 dB. Figure 7 shows the compensated open loop response.

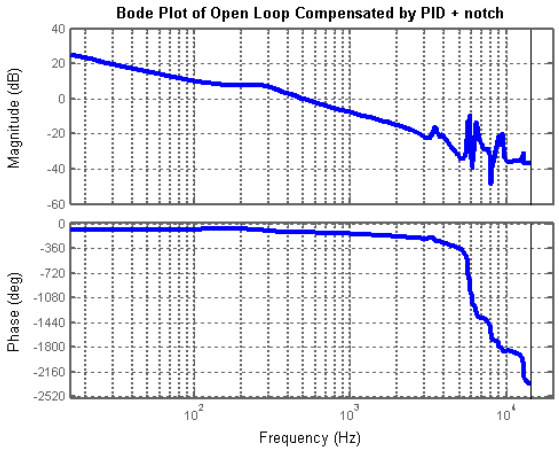

Figure 7 – Open loop of PID + notch

Both the standard PSD with real lag and the PSD with complex lag proceeded iteratively. First a candidate primary crossover 0 dB crossover frequency is selected, and the gain and the natural frequency of the PID compensator are chosen to achieve this crossover frequency with 60 degrees of primary phase margin. Then the real or complex lag was chosen to achieve 60 degrees of secondary phase margin while maintaining the original primary 0 dB crossover frequency. The phase loss introduced by the lag requires

reduction of the original primary 0 dB crossover and/or a reduction the original natural frequency of the PID compensator. With the new PID compensator and new crossover frequency, a new lag is chosen. the process of modifying the PID compensator and the lag is repeated until the primary 0 dB crossover is as large as possible while both the primary and secondary phase margins are 60 degrees.

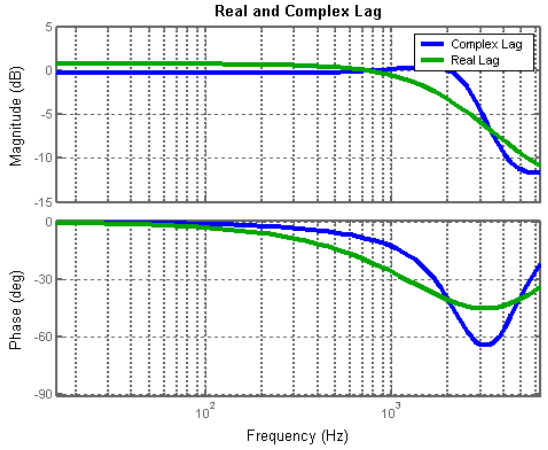

Figure 8 – Frequency responses of lag compensators

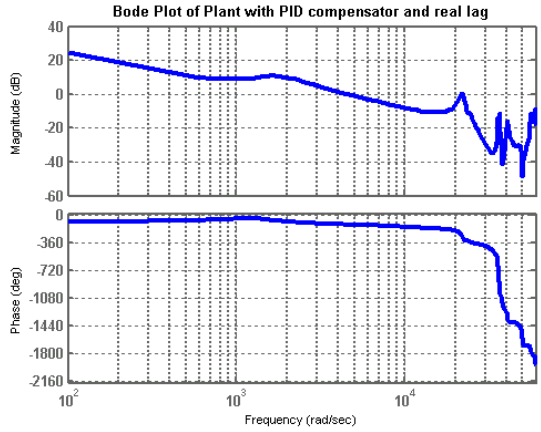

Figure 9 – Open loop of PSD with real lag

The standard PSD achieved a primary 0 dB crossover frequency of 730 Hz with a PID natural frequency of 175 Hz and a double lag compensator providing 45 degrees of phase loss at 3,183 Hz. Figure 8 shows lag compensator frequency response. Figure 9 shows the Bode plot of the compensated open loop, and Figure 10 shows the Nyquist plot. The actual primary phase margin is slightly smaller than 60 degrees, and the actual secondary phase margin is in slightly larger than 60 degrees. The reason is that to the phase loss caused by the computation delay was not accounted for during the design, but was accounted for during the performance evaluation and simulation.

The complex lag compensator provides another degree of freedom for the PSD. For a phase lag of φ at frequency ω_{lag}, the complex conjugate poles lie on a circle of radius $|p+z|/2$ and center $(z-p)/2$, where $z=\omega_{lag}/\sqrt{a}$, $p=\omega_{lag}\sqrt{a}$, and $a=(1-\sin\varphi/2)/(1+\sin\varphi/2)$. The complex conjugate zeros lie on a circle of the same radius but with center $(p-z)/2$. Both the poles and the zeros have the same damping ratio, which is the free parameter of the compensator. Figure 11 shows the pole zero map for a lag of 64.5 degrees at 3,183 Hz and damping ratio 0.5. As the damping ratio decreases, the maximum lag remains constant, but the phase notch narrows, the transition from low frequency to high frequency gain increases, while the difference between the low frequency and high frequency gain decreases. As the damping ratio decreases below 0.707, the magnitude response begins to resemble a node/anti-node pair. The reader is referred to [4] for the development and further discussion of the properties.

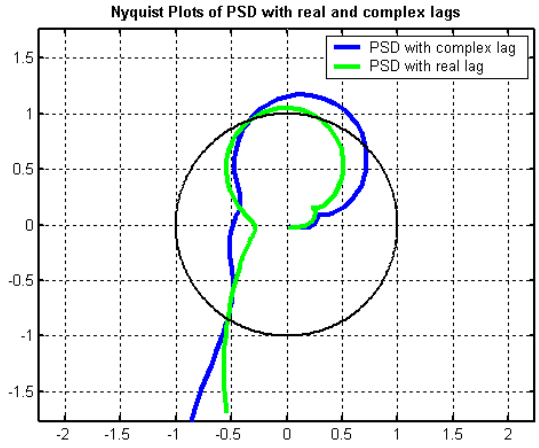

Figure 10 – Nyquist plot of PSD with real lag and complex lag

The procedure for the PSD with complex lag is the same as that for the PSD with real lag, except that the damping ratio is also decreased during the iteration. Decreasing the damping ratio reduces the effect of the complex lag on the primary phase margin, but also reduce the effect of the magnitude at the compensation frequency. The PSD with complex lag achieved a primary 0 dB crossover of 830 Hz with a PID natural frequency of 263 rad/s and a complex lag with damping ratio of 0.5 providing 64.5 degrees of phase loss at 3183 Hz. Figure 8 shows the complex lag compensator frequency response. Figure 12 shows the Bode plot of the compensated open loop, and Figure 10 shows the Nyquist plot. While the minimum distance from the –1 point to the graph is less than that for the PSD with real lag, the secondary phase margin is larger. Also, the larger excursion from the unit circle, where the angle from the negative real axis is more than 60 degrees, will result in greater disturbance rejection.

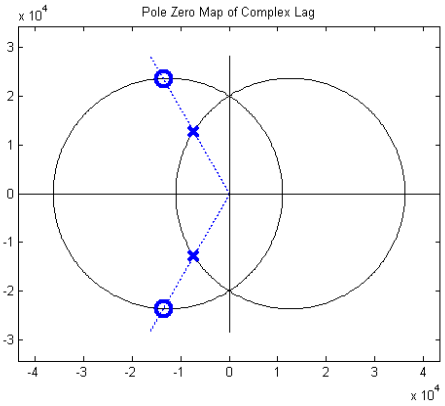

Figure 11 – Pole zero map of complex lag with damping ratio 0.5

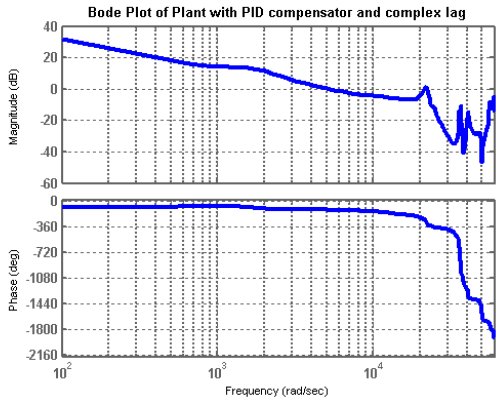

Figure 12 – Open loop of PSD with complex lag

IV. PERFORMANCE COMPARISON

The servo-positioning system of a HDD must keep the head as close as possible to the track center, in spite of RRO, NRRO, and disturbances acting on the VCM, such as external vibrations, etc. The tracking controller must provide fast access to adjacent tracks. Therefore, a fair comparison of the performance of different controllers requires the evaluation of both frequency responses and time responses, under realistic operating conditions.

Figure 13 and Figure 14 show the sensitivity functions and complementary sensitivity functions. The sensitivity function shows that the PSD with complex lag has a higher output disturbance rejection up to 1.2 kHz, compared with the other two controllers. The PSD with real lag has a peak at the first resonant frequency of the VCM, with a 5 dB magnitude. The PSD with complex lag, instead, has a 6 dB peak at 2 kHz, while the gain goes down around the resonance. This profile improves the performance of the servo system in terms of tracking capabilities. With respect to the input-to-output response, the PSD with complex lag exhibits a flat frequency response up to 3 kHz, and implying a fast response with little residual. The PID with notch shows a bandwidth of about 500 Hz, and so a much slower response to track-to-track commands is expected. The PSD with real lag has a bandwidth of about 1400 Hz and a peak around the first resonant mode. This will result in a slower response with wider residual oscillations, compared to the PSD with complex lag.

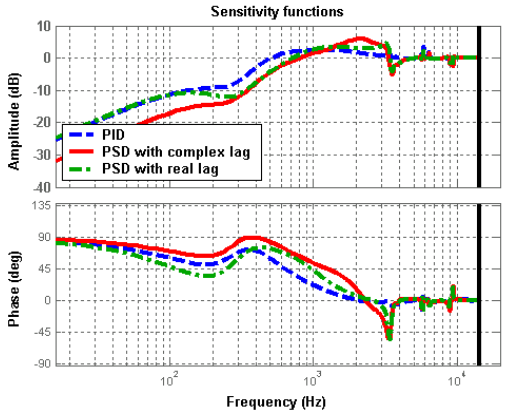

Figure 13 – Sensitivity functions for PID with notch (dash-dot), PSD with real lag (dashed) and PSD with complex lag (solid)

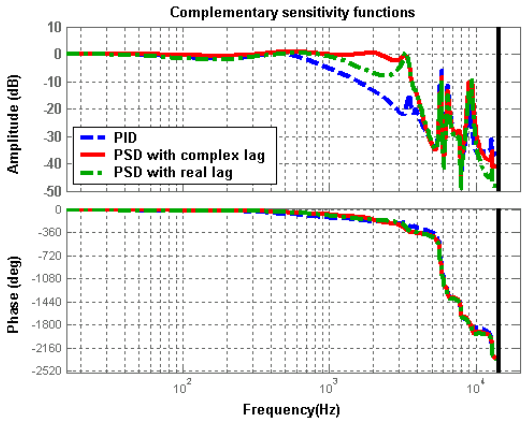

Figure 14 – Complementary sensitivity functions for PID with notch (dash-dot), PSD with real lag (dashed) and PSD with complex lag (solid)

Figure 15 shows the step responses of the three controllers, and they confirm the conclusions above. The PSD with complex lag reaches at the target track (with 5% of tolerance) in 2 ms, while the PID with notch and the PSD with real lag need 2.5 ms and 3 ms, respectively. The PSD with complex lag exhibits smaller residual vibrations, compared to the PSD with real lag.

During track-following operations, external disturbances can move the head off track. Such disturbances can be modelled as disturbance torques acting at VCM input , and may be caused either by the motion of the HDD body, as in mobile applications or RAID systems, or by the vibration of an unbalanced spindle motor. Figure 16 shows the response of the servo system to an step impulsive disturbance torque, applied at the VCM input during track following. The results show that PSD with complex lag provides the fastest recovery at the target position.

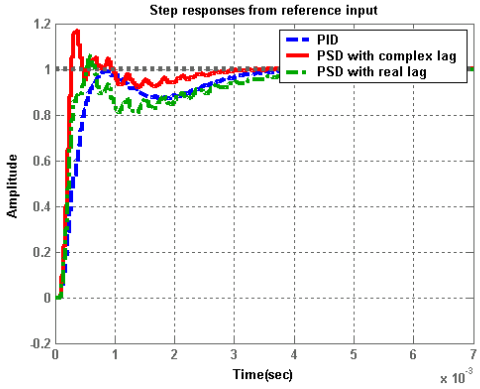

Figure 15 – Step responses the for PID with notch (dash-dot), PSD with real lag (dashed) and PSD with complex lag (solid)

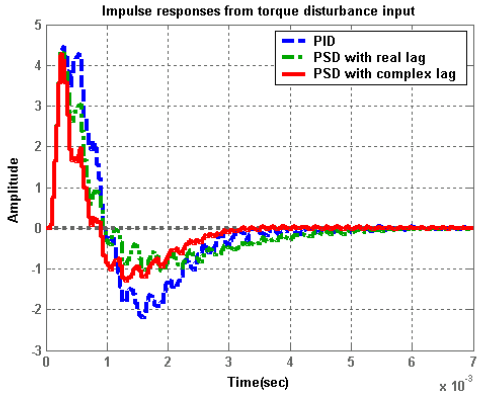

Figure 16 – Impulse torque disturbance response for PID with notch (dash-dot), PSD with real lag (dashed) and PSD with complex lag (solid)

Actual track profile, windage and disturbance data were obtained from the system described in Section II and used as inputs in simulations [6]. The resulting PES signals are shown in Fig. 17, and they confirm the superiority of the PSD with complex lag in keeping the head on the track center, in spite of RROs, NRROs and disturbances. The maximum and standard deviations from track center for the three controller are reported in Table 3. The table clearly shows that the PSD with complex lag is superior to the other controllers, achieving higher bandwidth, faster response, better rejection and more accurate tracking.

V. Conclusion

This paper compared PID plus notch, PSD with real lag, and PSD with complex lag as methods for designing controllers for a disk drive head positioning servo. The comparison showed that the properties of the complex lag compensator enable the PSD employing it to significantly outperform the other two approaches with respect to closed loop bandwidth, 0 dB sensitivity function crossover, step response, disturbance recovery time, and rejection of repetitive and broadband disturbances. Future work will further optimize the designs considered here through the use of the Sbode plot [5] and will implement these controllers on an experimental disk drive system.

This work was supported in part by NSF Grant number ECS-0072752

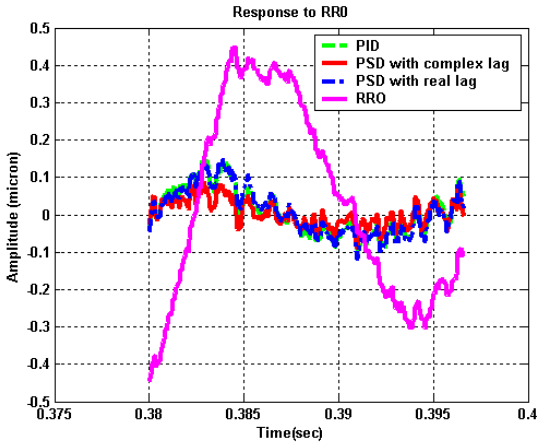

Figure 17 – Typical position error for PID with notch (dash-dot), PSD with real lag (dashed) and PSD with complex lag (solid)

TABLE III
CONTROLLERS PERFORMANCE

Controller ⇒ / Value⇓	PID + Notch	PSD + real lag	PSD + Complex lag
Closed loop BW	500 Hz	1400 Hz	3000 Hz
0 dB sensitivity cross	500 Hz	720 Hz	800 Hz
Sensitivity peak	3.5 dB	5.0 dB	6.0 dB
Step response time	2.5 ms	3.0 ms	2.0 ms
Dist. recovery time	4.5 ms	5.0 ms	3.0 ms
Max deviation	0.188	0.183	0.122
STD deviation	0.043	0.042	0.029

References

[1] M. Kobayashi, S. Nakagawa, and S. Nakamura. "A phase-stabilized servo controller for dual-stage actuators in hard disk drives," IEEE Transactions on Magnetics, v.39 n.2 , March 2003, pp. 844 –850

[2] R. Oboe, A. Beghi, P. Capretta, and F.C Soldavini. "A simulation and control design environment for single-stage and dual-stage hard disk drives"; IEEE/ASME Transactions on Mechatronics, v.7, n.2, June 2002, pp. 161 -170

[3] G.F. Franklin, J.D. Powell, and A. Emani-Naeini. Feedback Control of Dynamic Systems. Addison-Wesley, Reading, Massachusetts, Third edition, 1994

[4] W. Messner. "The Development, Properties, and Application of the Complex Phase Lead Compensator ," Proceedings of the 2000 American Controls Conference, Chicago, IL, 28-30 July 2000, pp. 2621-6 vol.4.

[5] W. Messner. "Some Advances in Loop Shaping with Applications to Disk Drives," IEEE Transactions on Magnetics, Vol. 37, No. 2, Mar 2001, pp. 651-6.

[6] M. Rotunno, M.E. Crowder, R. Oboe, R.A. de Callafon, "Determination of the Windage Induced Disturbance Spectrum in a Commercial Hard Disk Drive" – Proceedings of Information Storage and Processing Systems ISPS 2002 – Santa Clara (USA) – June 2002